Role of bonding, reduced screening, and structure in the high-temperature superconductors

C. Falter, M. Klenner, and Q. Chen
Institut für Theoretische Physik II, Festkörperphysik, University Münster, Wilhelm Klemm Strasse 10, 48149 Münster, Germany
(Received 22 June 1993)

In this paper we have studied the role of bonding, reduced screening, and structure in high-temperature superconductors (HTSC) using La_2CuO_4 as a prototype material. In addition to the ionic and metallic component of bonding recently investigated, we estimate the influence of covalence effects on the structural parameters and the phonon spectrum. Also, the effect of a reduced dispersion of the electronic band structure on the polarizability and the phonon frequencies is considered and (hypothetical) mechanisms are investigated, which would favor ferroelectricity in the HTSC. In a further topic we deal with reduced screening, introduced by nonadiabatic effects related to the quasi-two-dimensional band structure and its consequence for the electron-phonon interaction, the phonon dispersion, and the pairing mechanism. We then focus our interest on features related to the tetragonal-to-orthorhombic phase transition in La_2CuO_4. Structural parameters are calculated and the influence of the transition on the phonon dispersion as well as on the phonon-induced charge fluctuations is discussed. Finally, we present, on the basis of nonlocal electron-phonon interaction of the charge-fluctuation type, a theoretical interpretation of a universal relationship between T_c and the hole content in the HTSC.

I. INTRODUCTION

In the high-temperature superconductors (HTSC), mainly due to their structure, an unusual combination of ionic, metallic, and covalent bonding is realized. On the way to an understanding of the mechanism of the superconductivity in these materials one first needs information on their structural, electronic, magnetic, and other normal-state properties. Referring to this an enormous amount of experimental and theoretical work has been carried out until now.

In many investigations, resting on the Hubbard-Hamiltonian, a pure electronic or magnetic rather than the conventional electron-phonon mechanism is thought to be the key for an understanding of the superconductivity. The Hubbard model is probably the simplest model which accounts for electronic correlations approximatively. In this model the competition between chemical bonding (hopping of electrons) and Coulomb repulsion between two electrons on the same atom decides the behavior of mobile charge carriers. So it is quite natural and useful to study (at least in principle) the influence of strong electronic correlations in the CuO plane and to estimate in particular their effect on the single-particle excitations in the vicinity of the Fermi surface within this model. However, when relating such a model definitely to the HTSC several facts should be considered in judging its degree of realism with respect to that application. The selection of the relevant electronic degrees of freedom (t-J model, three-band model, etc.) and of the space dimension must be adequate. For example, coupling of the CuO layers should be important in this context. Furthermore, one should note that the Hubbard model is with respect to the Coulomb interactions a short-range model ignoring the long-range character of the latter, which, on the other hand, is important in the HTSC being metals at the limit to an ionic insulator. The only place where some kind of long-range character is introduced effectively into the model is via the antisymmetrization of the wave function. Finally, the specific crystal structure of these compounds favoring strong ionic forces is not considered. On the other hand, precisely these Coulomb contributions are crucial to the appearance of the unusual nonlocal, long-range electron-phonon interaction (EPI) effects in these materials.[1–5]

From estimates which are exclusively based on local EPI effects the electron-phonon mechanism was thought to be not strong enough to contribute substantially to the high-T_c values. However, such considerations ignore the nonlocal long-range EPI effects which recently have been shown to reinforce the phonon-mediated contribution to pair binding[2,3] by leading to a large electron-phonon coupling which has also been confirmed by self-consistent linearized-augmented-plane-wave (LAPW) calculations within the local-density-functional approximation (LDA).[4] These results do not, of course, rule out possible contributions from an electronic mechanism to high-temperature superconductivity, but emphasize contributions via electron-phonon coupling which are unique for the HTSC and which are not present in conventional metals and superconductors displaying good metallic screening in all directions of space.

From the experimental side it can be concluded quite generally that theories which are inconsistent with a Fermi surface can be ruled out.[6] The experiments essentially are in agreement with the Fermi-surface predictions of LDA band-structure calculations[1,6] and this speaks in favor of the Fermi-liquid picture. The fact that the LDA does not lead to the insulating ground state for the undoped compounds does not invalidate from the outset its application for the doped metallic phase. Note on this matter that recent self-interaction corrected local-spin-density calculations for La_2CuO_4 (Ref. 7) are in agreement with the experimentally observed antiferromagnetic

0163-1829/93/48(22)/16690(17)/$06.00

and insulating ground state. There is also a steady growing evidence from the experimental side for strong electron-phonon coupling in the HTSC, see Refs. 1, 4, and 8, and references therein. So it is quite natural to investigate the electron-phonon interaction in the HTSC and to separate features which are normal from those which are unique and really important and if possible to relate these to structural and electronic properties which are characteristic for these compounds. Such attempts have been undertaken in Refs. 1–5. In particular, the calculations in Refs. 2 and 3 indicate that the unusual strong nonlocal EPI effects are a consequence of an intricate interplay of the crystal structure, the quasi-two-dimensionality of the electronic structure, the strong ionic forces, and a specific type of weak screening dominated by ionic charge fluctuations and strong localization features of the electrons dictated by the Coulomb interaction. Finally, nonadiabatic effects can further reduce the screening for certain phonons in the (0,0,1) direction.

In the present work we use the same density response description as in Refs. 2 and 3. The local part of the electronic density response will be approximated by a proper *ab initio* model of rigid ions to describe the important effects of the ionic component of bonding. Using such a model as a reference system, nonlocal contributions to the density response are additionally taken into account in the form of charge fluctuations on the ions. Our calculations for the tetragonal phase of La_2CuO_4 (Refs. 2 and 3) have demonstrated that the most important features of the experimental phonon spectrum can be understood within such an approach. We have also discussed the special and very important role of the symmetric apical oxygen breathing mode at the Z point (O_z^z) for electron (hole) pairing via nonlocal EPI. In this vibration and to a lesser extent also for La_z^z nonlocal EPI effects of charge-fluctuation type accompanied by corresponding changes of the crystal potential of a uniform sign in the CuO plane have been shown to generate in the metallic phase of La_2CuO_4 an interplane charge transfer which leads to a strong renormalization of O_z^z when compared to the insulating phase. In the latter the charge transfer is restricted locally within the plane and long-range charge transfer is not possible as in the metallic phase. This leads to a less effective screening and to very large changes of a uniform sign of the phonon-induced potential in the CuO layer for this mode[3] (by more than a factor of 5 as compared with the metal).

Such a drastic suppression of the screening of the phonon-induced changes of the crystal potential for Λ phonons and especially for O_z^z can also be expected in the metallic phase in case nonadiabatic electron-phonon coupling would be important, which is likely to be the case if the dispersion of the electronic bands in c direction is sufficiently small. In such a situation changes of the potential in the CuO plane as large as those obtained for the insulating phase can also result in the metallic phase. Simultaneously, these nonadiabatic effects would strongly reinforce the attraction of holes (electrons) via the nonlocal pairing mechanism as discussed in Refs. 2 and 3. In La_2CuO_4, however, the experimental findings, i.e., the vanishing of the "ferroelectric split" in the metallic phase and the related appearance of a corresponding Λ_1 branch with a very steep dispersion,[3] suggest that the adiabatic approximation should just be valid in this material. This conclusion is also supported by the dispersion of the electronic band structure in the c direction which is of the order 0.5 eV for many bands as shown in the calculation in Ref. 1 and this has to be compared with the high-frequency phonons of about 80 meV. On the other hand, if the dispersion of the electrons in the c direction, in particular for the band at the Fermi level, would be small enough, nonadiabatic effects of the type above are to be expected for high-frequency phonons with wave vectors in the (0,0,1) direction. Such a situation could be realized in YBaCuO where the adiabatic approximation might break down for some phonons in the (0,0,1) direction as qualitatively discussed in Ref. 5. The same thing could happen in the recently discovered superconductor $HgBa_2CuO_4$ (because of the larger distance between the planes) with only one CuO layer per unit cell but with a very high-T_c value of 94 K.[9] In both cases the nonadiabatic enhancement of the phonon-induced potential in the CuO plane will strengthen the nonlocal pairing mechanism significantly and may lead to the higher T_c values.

Thus, quite generally we recognize the important role played by certain charge-fluctuation patterns and corresponding changes in the crystal potential induced by definite phonon modes, like O_z^z in the case of La_2CuO_4, for phonon renormalization and nonlocal electron-phonon interaction strengthening phonon-mediated pair binding. Having these facts in mind, it is important to look for similar significant phonon modes in the other HTSC generating possibly similar favorable charge-fluctuation patterns. The existence of such patterns in other HTSC can indeed be confirmed as our preliminary calculations in $YBa_2Cu_3O_7$ indicate.[10,11]

In case of La_2CuO_4 for the same reason it is interesting to investigate the variations of the charge-fluctuations induced by the structural transition from the tetragonal to the orthorhombic phase, i.e., the influence of the tilt, especially for the O_z^z and La_z^z modes. These calculations might also be helpful in the discussion of the relation between the occurrence of superconductivity in Ba- or Sr-doped La_2CuO_4 and subtle structural changes. Such a relationship together with the question if orthorhombicity of the crystal is a crucial condition for giving cause for high-T_c superconductivity is an active area of experimental research.[12–16]

The remainder of the paper is organized as follows. In Sec. II, the theoretical formalism is reviewed. Section III is concerned with the tetragonal phase of La_2CuO_4. In addition to our calculations in Refs. 2 and 3 we give an estimate within a simple model of the influence of covalence effects on the structural parameters and the phonon dispersion. Then, the influence on the electronic polarizability and the phonon dispersion produced by a possible narrowing of the antibonding band is investigated within our model for the electronic band structure. Such a discussion could be of some interest because quantum Monte Carlo calculations[17] for the three-band Hubbard model yield a smaller Fermi velocity and bandwidth in comparison with LDA calculations and show good agree-

ment with the experiments for both the Fermi velocity and the location of the Fermi surface. Further, we study in this section hypothetical microscopic mechanisms which would allow for a softening of the "ferroelectric mode" in La_2CuO_4. These studies might be useful for the interpretation of a phase-transition-like feature as recently discussed in Ref. 18 for the quantum paraelectric regime of $SrTiO_3$ and could also be of relevance for the occurrence of incommensurate phases in the HTSC. Finally, we present in this section a nonadiabatic model calculation of the phonon dispersion in order to demonstrate the way the reduced screening related to the quasi-two-dimensional electronic structure would change certain phonon modes via a nonadiabatic electronic density response. Section IV deals with changes of the structural properties and the phonon spectrum brought about by the phase transition from the tetragonal to the orthorhombic phase. In Sec. V, we investigate the relationship between charge fluctuations and tilting and discuss the possible role of orthorhombicity from this point of view. Section VI provides an interpretation on the basis of the nonlocal EPI effects of charge-fluctuation type of a universal relation between the ratio $T_c/T_{c,\max}$ and the hole content in the HTSC, recently established by an analysis of experimental data.[19] In Sec. VII, the main points of the paper are summarized.

II. THEORETICAL METHOD

In this section we present a condensed review of the theoretical method used in our calculations. More details can be found in Refs. 2 and 3. As already mentioned in the Introduction, the local part of the electronic density response is approximated by a proper *ab initio* model of rigid ions to represent the important effects of the ionic forces in the crystal. The ionic densities $\rho_\alpha(\mathbf{r}-\mathbf{R}^{\mathbf{A}})$ ($\mathbf{R}^{\mathbf{A}}=\mathbf{R}^{\mathbf{a}}+\mathbf{R}^{\alpha}$ denote the centers of localization of the ions and $\mathbf{a},\alpha$ are the primitive and nonprimitive lattice indices, respectively) have been calculated with a modified version of the Herman-Skillman program[20] where the Slater exchange potential has been replaced by the exchange potential of local-density-functional theory and a correlation potential according to Ref. 21 has been used additionally. The unstable O^{2-} ion is treated with the help of the Watson-sphere method.[22] With such ionic densities, the interactions between the ions are calculated using the approach of Ref. 23. This procedure results in pair potentials $\Phi_{\alpha\beta}(R)$ between ions of type α and β at a distance R:

$$\Phi_{\alpha\beta}(R)=\frac{Z_\alpha Z_\beta}{R}+\tilde{\Phi}_{\alpha\beta}(R) . \tag{1}$$

Z_α, Z_β are the ionic charges, and the long-range Coulomb contribution has been separated from the short-range part $\tilde{\Phi}$. The latter quantity is calculated numerically for different values of the distance R between the ions and the results are fitted to a two-exponential form for convenience:

$$\tilde{\Phi}(R)=\alpha_+ e^{-\beta_+ R}-\alpha_- e^{-\beta_- R} . \tag{2}$$

Differentiating $\Phi_{\alpha\beta}$ twice with respect to the ion coordinates yields the force constants from which the dynamical matrix of our ionic reference model is obtained by Fourier transformation. Finally, the energy of the ionic system is given by

$$E=\frac{1}{2}{\sum_{\mathbf{b},\alpha,\beta}}' \Phi_{\alpha\beta}(|\mathbf{R}^{\mathbf{b}}_\beta-\mathbf{R}^{\mathbf{O}}_\alpha|) . \tag{3}$$

E is minimized in our calculations with respect to the relevant structure parameters of the crystal in order to get the optimized distances of each ion pair in the model. In the case of the tetragonal phase of La_2CuO_4, for instance, the structure parameters are the lattice constant a, the ratio of the c axis to the lattice constant c/a, and the positions of La and O_z in the elementary cell z(La), $z(O_z)$.

So far the local part of the electronic density response has been accounted for by the ionic *ab initio* model. Beyond this approximation we additionally include nonlocal contributions to the density response in the form of electronic charge fluctuations on the ions. For a detailed description of the electronic density response and the electron-phonon interaction in terms of these charge fluctuations and for a derivation of how these fluctuations enter the dynamical matrix and the matrix elements of the electron-phonon interaction, we refer to Refs. 2 and 3. In the following we present only the key elements of such a formulation and give their physical meaning.

The fundamental quantities which determine the electronic density response are the quantities $B_i^{\mathbf{b}\kappa\mathbf{A}}$, which express the "force" on the charge fluctuation at $\mathbf{R}^{\mathbf{b}}_\kappa$ with form factor $\rho^{\mathbf{b}}_\kappa$ if ion $\mathbf{A}$ is displaced in the i direction and the corresponding change in energy $C^{\mathbf{ab}}_{\kappa\kappa'}$ in case such charge fluctuations have been excited at the positions $\mathbf{R}^{\mathbf{a}}_\kappa$ and $\mathbf{R}^{\mathbf{b}}_{\kappa'}$ in the solid. In the framework of density-functional theory we obtain

$$B_i^{\mathbf{b}\kappa\mathbf{A}}=\int dV \rho_\kappa(\mathbf{r}-\mathbf{R}^{\mathbf{b}}_\kappa) V_i^\alpha(\mathbf{r}-\mathbf{R}^{\mathbf{A}}) \tag{4}$$

with

$$V_i^\alpha(\mathbf{r}-\mathbf{R}^{\mathbf{A}})=\frac{\partial}{\partial R_i^{\mathbf{A}}} V_\alpha(\mathbf{r}-\mathbf{R}^{\mathbf{A}}) , \tag{5}$$

where $V_\alpha(\mathbf{r}-\mathbf{R}^{\mathbf{A}})$ is the ionic potential,

$$C^{\mathbf{ab}}_{\kappa\kappa'}=\int dV\, dV' \rho_\kappa(\mathbf{r}-\mathbf{R}^{\mathbf{a}}_\kappa) F''(\mathbf{r},\mathbf{r}') \rho_{\kappa'}(\mathbf{r}'-R^{\mathbf{b}}_{\kappa'}) \tag{6}$$

with

$$F''(\mathbf{r},\mathbf{r}')=T_s''(\mathbf{r},\mathbf{r}')+v(\mathbf{r}-\mathbf{r}')-v_{xc}(\mathbf{r},\mathbf{r}') . \tag{7}$$

In this equation v is the Coulomb interaction, T_s'' and $(-v_{xc})=E_{xc}''$ are the second functional derivatives with respect to the density ρ of the kinetic energy and the exchange-correlation energy. Introducing the inverse polarizability π^{-1} of the electronic system by the relation $\pi^{-1}(\mathbf{r},\mathbf{r}')=T_s''(\mathbf{r},\mathbf{r}')$, we can express C in Eq. (6) in compact notation as

$$C=\pi^{-1}+\tilde{V} , \quad \tilde{V}=V-V_{xc} . \tag{8}$$

The contribution of the kinetic energy enters via the po-

larizability π. The latter quantity is approximated within a tight-binding representation as described in detail in Ref. 3, allowing for charge fluctuations on the Cu and the $O_{x,y}$ ions in the CuO plane. In full notation it can be written in this case as

$$\pi_{\kappa\kappa'}(\mathbf{q}) = -\frac{2}{N}\sum_{\substack{n,n'\\ \mathbf{k}}} \frac{f_n(\mathbf{k}) - f_{n'}(\mathbf{k}+\mathbf{q})}{E_n(\mathbf{k}) - E_{n'}(\mathbf{k}+\mathbf{q})} \times [C^*_{\kappa n}(\mathbf{k}) C_{\kappa n'}(\mathbf{k}+\mathbf{q})] \times [C^*_{\kappa' n}(\mathbf{k}) C_{\kappa' n'}(\mathbf{k}+\mathbf{q})]^* \ . \quad (9)$$

The f's, E's, and C's represent occupation numbers, the electronic band structure, and the expansion coefficients of the Bloch functions in terms of tight-binding functions. $\mathbf{k}$ and $\mathbf{q}$ are wave vectors from the first Brillouin zone. For the calculation of $\pi_{\kappa\kappa'}(\mathbf{q})$ we use the same two-dimensional tight-binding model for the band structure as in Refs. 2 and 3.

The important long-range Coulomb contributions of B and C can be separated, i.e.,

$$[B_i^{b\kappa A}]_c = \frac{\partial}{\partial R_i^{\,A}} \left[\frac{Z_\alpha}{|\mathbf{R}^{A} - \mathbf{R}^{b}_{\kappa}|} \right] , \quad (10)$$

$$[C^{ab}_{\kappa\kappa'}]_c = \frac{1}{|\mathbf{R}^{b}_{\kappa'} - \mathbf{R}^{a}_{\kappa}|} , \quad (11)$$

and can be dealt with exactly using the Ewald method. The short-range contribution to the charge-fluctuation-ion coupling B and to the "potential-energy" part $\tilde{V}$ in Eq. (8) are calculated approximatively using for the form factors the Cu d and O p orbital densities. In such a procedure it is assumed that the charge fluctuation at an ion corresponds in a first approximation to a change of the occupation of its outmost shell. Thus, the $\tilde{V}$'s and B's can be estimated by calculating the occupation-dependent Hartree and XC energy of an ion (in the local-density approximation) and the occupation-dependent pair potential $\tilde{\Phi}_{\alpha\beta}$ of a pair of ions. The most important contribution to $\tilde{V}$ is given by the on-site repulsion terms $\tilde{V}^{aa}_{\kappa\kappa}$, in particular, at the Cu ion, affecting to a large extent the magnitude of the charge fluctuations. The latter, after having been excited via B, are determined by the interplay of the kinetic- and potential-energy contributions in Eq. (8) as discussed in detail in Ref. 3.

Finally, in order to distinguish the density response in the insulating phase from that in the metallic phase we use a criterion which expresses the different analytic behavior in both phases of the polarizability in the long-wavelength limit ($\mathbf{q}\to 0$). In our formulation of the density response this criterion can be written as[2,3]

$$\sum_{\kappa,\kappa'} \pi_{\kappa\kappa'}(\mathbf{q}\to 0) = \begin{cases} O(q^2) \text{ insulator} , \\ Z(E_F) \text{ metal} \end{cases} \quad (12a)$$

and

$$\sum_{\kappa'} \pi_{\kappa\kappa'}(\mathbf{q}\to 0) = O(q) \text{ insulator} , \quad (12b)$$

while the expression on the left-hand side in Eq. (12b) is different from zero in the case of a metal. $Z(E_F)$ means the density of states at the Fermi level.

III. La_2CuO_4 IN THE TETRAGONAL PHASE

We refer to the calculations for La_2CuO_4 in Refs. 2 and 3 and estimate additionally the influence of covalence effects on the structural parameters and the phonon dispersion in the tetragonal phase of this material. Furthermore, the effect on the polarizability and the phonon dispersion of a possible narrowing of the electronic band structure is investigated. Then (hypothetical) microscopic mechanisms are considered which would be favorable for a softening of the "ferroelectric mode" in La_2CuO_4. Finally, nonadiabatic effects on the phonon dispersion are studied.

Our results[3] for the structure parameters of tetragonal La_2CuO_4 in the ionic model (denoted as FKL in Table I), which have been obtained from the minimization of the energy in Eq. (3) using nominal charges for the ions, i.e., La^{3+}, Cu^{2+}, and O^{2-}, indicate an enhanced planar lattice constant and a too small (c/a) ratio in comparison with the experiments.[24] This can be considered to be a consequence of the use of spherical ions and the neglect of covalence effects leading to an overestimation of the overlap repulsion between Cu and $O_{x,y}$ ions in the plane. The agreement of the internal structure parameters $z(O_z)$ and z(La) with the experimental values is in the case of La perfect and also satisfying for O_z confirming the validity of the ionic description of these ions, with the minor restriction that O_z might be considered to be slightly more covalent than La. Further, the experimental Cu-$O_{x,y}$ interatomic distance (~ 1.9 Å) turns out to be smaller than the sum of the ionic radii of Cu^{2+} and $O^{2-}_{x,y}$ (Ref. 25) indicating a certain contribution of covalency to the bonding in the plane.

In order to estimate the influence of covalency within a simple model we use an ansatz of the form

$$E^{\alpha\beta}_{\text{cov}} = -c \int dV [\tilde{\rho}_\alpha(\mathbf{r}) \tilde{\rho}_\beta(\mathbf{r}-\mathbf{R})]^{1/2} \quad (13)$$

to simulate the fact that covalency leads to an attraction and is governed by the overlap for large separations. In the model denoted as $E_{\text{cov}} \neq 0$ in Table I such a term is added to the pair potential $\tilde{\Phi}_{\alpha\beta}$ in Eq. (1) before the energy minimization is carried through. c in Eq. (13) is a positive constant and $\tilde{\rho}_\alpha, \tilde{\rho}_\beta$ are the valence charge densities of the ions of type α or β, respectively. For numerical reasons this contribution to the pair potential is fitted to an additional exponential function $(-\alpha e^{-\beta R})$ in the vi-

TABLE I. Structure parameters for tetragonal La_2CuO_4 as obtained from the energy minimization for different models described in the text. The experimental results are from Ref. 24.

	a (Å)	c/a	$z(O_z)$	z(La)
$E_{\text{cov}} \neq 0$	3.691	3.376	0.189	0.362
$E_{\text{cov}} = 0$	3.978	3.055	0.192	0.363
FKL	3.979	3.018	0.190	0.363
Expt.	3.79	3.49	0.182	0.362

cinity of the interatomic distance. In our numerical calculations only the contributions of the nearest neighbors in the CuO plane are taken into account. Furthermore, we have replaced the nominal charges for Cu and $O_{x,y}$ used in the FKL model by effective ionic charges. As trial values we took $+1.6$ for Cu and -1.8 for $O_{x,y}$. This choice is guided by the procedure adopted in Ref. 26, where the self-consistent crystalline charge density of $YBa_2Cu_3O_7$ obtained from a LAPW calculation is compared with a model density of overlapping spherical ionic charge densities formed with different ionic configurations. In our fit to the exponential form above we then obtain $\alpha=2.114$ and $\beta=0.796$ (in atomic units) if c is chosen to be equal one.

With these values the energy minimization has been carried out. The resulting structure parameters are displayed in Table I together with those values which have been obtained from a calculation ignoring the contribution from Eq. (13) ($E_{\rm cov}=0$). Comparing the latter results with the FKL model, we see that taking effective ionic charges instead of their nominal values has only a minor effect on the structure parameters. On the other hand, the calculation including covalence effects ($E_{\rm cov}\neq 0$) leads to an improvement of the structure parameters. The planar lattice constant is significantly decreased by the covalent bonding in the plane in comparison with the pure ionic model and its value is now even smaller than the experimental one for the special choice for c. This indicates that the covalent contribution as chosen in our model overestimates the true covalent interaction between Cu and planar oxygen. Of course, one could adjust c in Eq. (13) and/or the values of the effective ionic charges, which have an implicit effect on covalency, in order to improve the agreement with the experimental results, but this is not our concern here.

The phonon dispersion curves of the models with $E_{\rm cov}=0$ and $E_{\rm cov}\neq 0$ are shown in Figs. 1(b) and 1(c), respectively. Comparing Fig. 1(b) with Fig. 1(a), which reproduces the results from Ref. 3 where nominal ionic charges have been used, we find that the number of unstable modes has increased by one, the B_{2u} mode at Γ comes down while the acoustic modes are now stable along the whole Δ direction. As far as the unstable vibrations in the ionic models are concerned these modes indicate physical properties like instabilities and/or anharmonicities in the tetragonal phase of La_2CuO_4 related to the important ionic component of the forces, see also Refs. 1 and 3. For example, at the X point the mode with the largest negative "frequency" is the rotation mode (B_{1g}) of the O_{xy} ions in the x-y plane. The next one with the second lowest "frequency" is the tilt mode (B_{2g}) followed by the B_{2u} sliding mode involving mainly O_z motion and to a lesser degree also La motion perpendicular to the c axis. Such a kind of sliding motion of O_z and La is also involved in the most unstable E_u mode at the Γ point. In self-consistent LAPW calculations[27,28] all these modes are found to be either unstable (tilt mode) or very anharmonic. This means that in the tetragonal high-temperature phase these latter modes are only stabilized by anharmonic interactions and harmonic models where these modes are found to be stable are at least questionable.

The instability of the tilt mode correctly predicts the phase transition from the tetragonal structure to the low-temperature orthorhombic structure observed experimentally. From the comparison of Figs. 1(b) and 1(c) we see that two unstable E_u modes and an E_g mode are remarkably stabilized by the covalence effect. On the other hand, the two E_u modes with the highest frequency in the ionic model are further increased which is a consequence of the too small planar lattice constant in the model (see Table I), leading for these planar CuO bond-stretching modes to a strong increase of the overlap repulsion which cannot be overcompensated by the covalent forces, at least in our model with our choice for c in Eq. (13). Comparing the results for the frequency of the "ferroelectric mode" we find that the latter is lower in the model using effective ionic charges and also in the model taking covalence effects into account than in the model using nominal ionic charges.

Next we study the effect on both the polarizability $\pi_{\kappa\kappa'}(\mathbf{q})$ from Eq. (9) and on the phonon dispersion produced by a narrowing of the antibonding band within the model for the electronic band structure used in Ref. 3. Such an investigation is motivated by quantum Monte Carlo calculations of single-particle excitations in the vicinity of the Fermi surface within a three-band Hubbard model[17] which yield a smaller Fermi velocity and bandwidth than LDA calculations. In Ref. 3 we have used for the calculation of $\pi_{\kappa\kappa'}(\mathbf{q})$ a two-dimensional tight-binding model for the band structure which is in qualitative agreement with the full three-dimensional LDA band structure. The basis set of this model consists of five $3d$ orbitals on the Cu and three $2p$ orbitals on each of the two planar oxygens (11-band model). The band structure and the corresponding polarizability of this model are shown in Figs. 2(a) and 2(b), respectively, see also Ref. 3 for a detailed discussion. In order to simulate the narrowing of the antibonding band in our model we have reduced the values of the tight-binding parameters $V_{pd\sigma}$ and $V_{pd\pi}$ by 50%. The new band structure with a narrowed antibonding band is displayed in Fig. 3(a). Using this band structure we have calculated from Eq. (9) the matrix elements $\pi_{\kappa\kappa'}(\mathbf{q})$ of the polarizability. The results are shown in Fig. 3(b). The comparison with Fig. 2(b) demonstrates that the main differences can be found in the dominant contribution $\pi_{11}(\mathbf{q})$ which arises from the diagonal Cu-Cu polarizability. We find an enhancement for $\pi_{11}(\mathbf{q})$ along all the symmetry directions considered, and the nesting peak at the M point (X point of the three-dimensional zone) of Fig. 2(b) is broadened significantly by the band narrowing. On the other hand, our calculation of the phonon dispersion using the new polarizability based on the narrowed antibonding band shows almost no changes from the old results given in Ref. 3. This may be due to the fact that the phonon frequencies are not directly related to the fine details of the band structure at the Fermi surface because the relevant quantity for the phonon-induced electronic density response contains (besides B) the quantity C from Eq. (8),

and this quantity involves both, band-structure effects via π and potential-energy effects via $\tilde{V}$, where the latter quantity controls the phonon renormalization in the case of the highly correlated electrons considered here to a large extent. Furthermore, by calculating π, a certain averaging of the total band structure is performed and the dispersion of the single-particle excitations in the vicinity of the Fermi surface enters the phonon frequencies only indirectly by intra- as well as interband transitions. In addition, there is a further weighting by the wave functions, see Eq. (9). In this context it is interesting to note that frozen-phonon calculations within the framework of density-functional theory are ground-state calculations of the total energy and thus also imply some

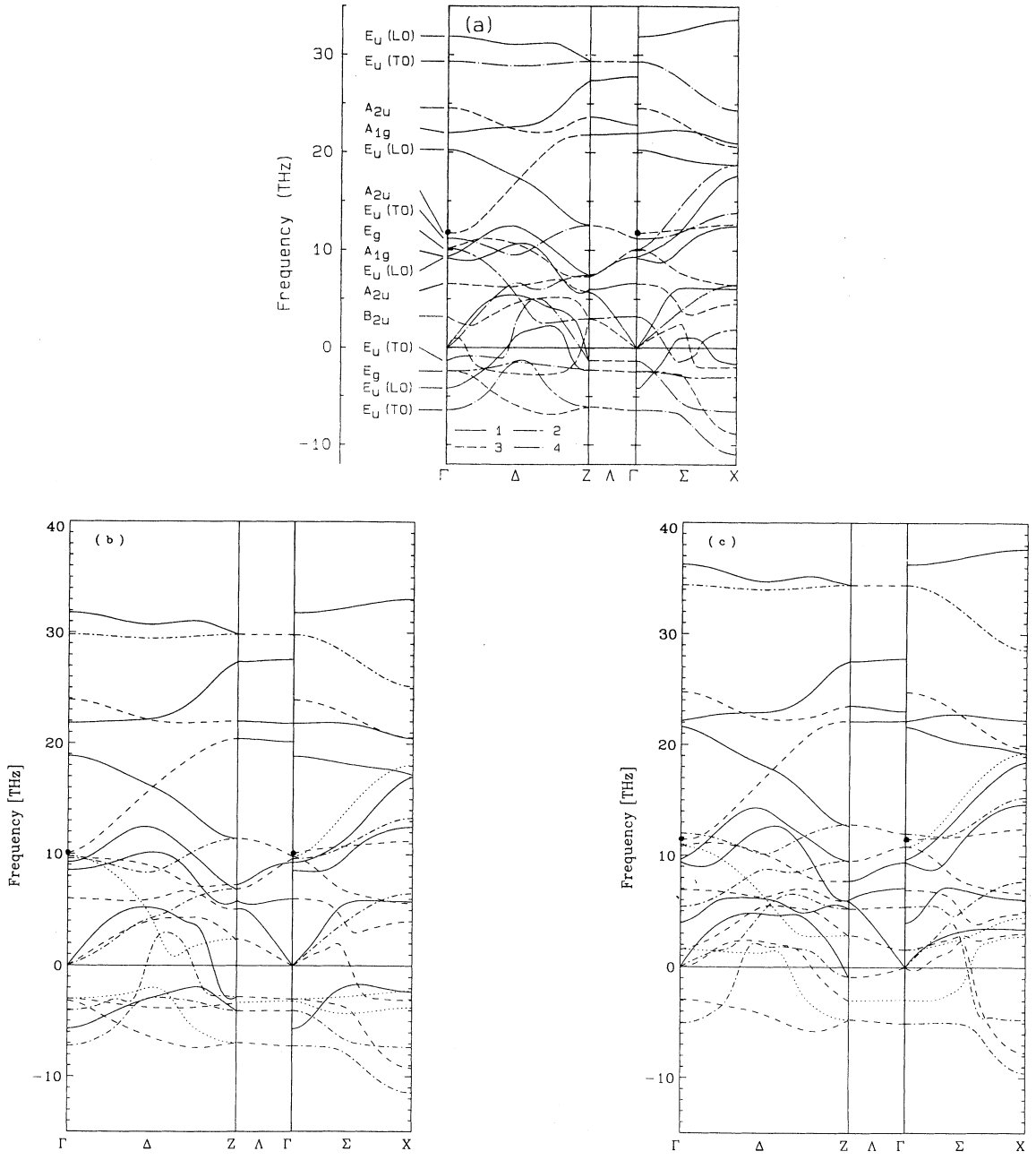

FIG. 1. Calculated phonon dispersion curves of tetragonal La_2CuO_4 for the ionic reference model using (a) nominal ionic charges and (b) using effective ionic charges $Cu^{1.6+}$, $O_{xy}^{1.8-}$, O_z^{2-}, La^{3+}. In (c) the latter ionic model is used and covalence effects are included according to Eq. (13). The dispersion is presented for the main symmetry directions $\Delta \sim (1,0,0)$, $\Lambda \sim (0,0,1)$, and $\Sigma \sim (1,1,0)$. The classification of the phonon branches by irreducible representations is brought about in the figure by using different line types (——, 1; · · · ·, 2; — — —, 3; —·—·—·, 4). Imaginary frequencies are represented as negative numbers. Note that in (a) the line type —-, 2 has been used as in Ref. 3 instead of · · · ·, 2. The single dots mark the "ferroelectric mode."

averaging over the (occupied) band structure. Again the one-particle excitations at the Fermi surface are only indirectly involved.

From our discussion of the unstable modes in the ionic model we see that as a consequence of the strong ionic forces La_2CuO_4 and presumedly the perovskite-derived high-T_c superconducting oxides in general display similar instabilities and anharmonic properties which can also be observed in other perovskites. For example, the tilt instability and the strong anharmonicity of the rotational mode is similar to rotational instabilities found in many perovskites. On the other hand, the "ferroelectric mode" is quite stable in La_2CuO_4, see Figs. 1 and 6, which, of course, is not the case for those perovskites displaying ferroelectricity. So it is tempting to think about microscopic mechanisms, i.e., specific bonding features, which would favor the tendency towards a ferroelectric instability in general.

The stability of the "ferroelectric mode" in La_2CuO_4 is mainly due to the strong short-range overlap repulsion between the ions. In the model with effective ionic charges [Fig. 1(b)] the balance between long-range Coulomb forces and short-range overlap repulsion has changed and the ferroelectric mode frequency of 11.73 THz in the model with nominal charges [Fig. 1(a)] is decreased to 10.06 THz. Also covalent hybridization effects which would additionally reduce the overlap repulsion are very likely to favor the trend towards ferroelectricity. This can only indirectly be confirmed by the results displayed in Fig. 1(c), where covalence effects according to Eq. (13) are taken into account because of the drastic decrease in the planar lattice constant which is inherent in this model. The frequency of the "ferroelectric mode" in this model is 11.49 THz, i.e., smaller than in the pure ionic model with nominal charges and with the large planar lattice constant. Assuming that the overlap repulsions would increase with decreasing lattice constant, the covalence effects in the model counteract this trend leading to a net reduction of the frequency.

However, the most dramatic softening of the "ferroelectric mode" can be achieved in case we implement axial dipolar fluctuations of the electronic density at the apex oxygen using the general density response approach developed in Refs. 2 and 3. The result is shown in Fig. 4 which displays the calculated dispersion of tetragonal La_2CuO_4 in the ionic model with nominal charges for the ions and including (hypothetically) the dipolar fluctuations just mentioned. A comparison with Fig. 1(a) demonstrates the dramatic and mode-specific influence of these fluctuations (11.73 THz$\rightarrow -5.2$ THz for the model

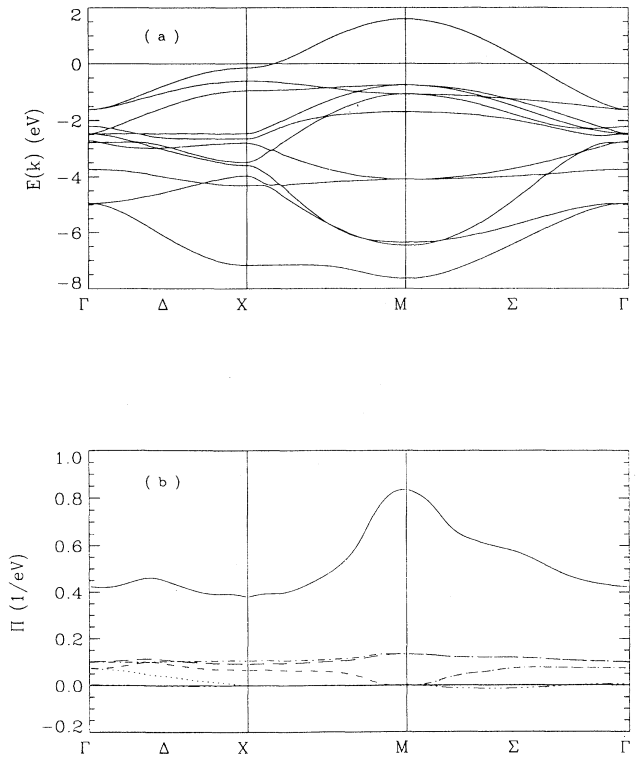

FIG. 2. (a) Electronic band structure of the two-dimensional 11-band tight-binding model used in Ref. 3. $\Delta\sim(1,0)$ and $\Sigma\sim(1,1)$ are symmetry directions of the two-dimensional Brillouin zone. The Fermi energy is normalized to zero. In (b) the dispersion of the matrix elements $\pi_{\kappa,\kappa'}(\mathbf{q})$ of the corresponding polarizability according to Eq. (9) is shown. The following line types have been used: ——, π_{11}; · · · ·, π_{12}; — — —, π_{13}; —·—·—·, π_{22}; —···—···, π_{23}; — — —, π_{33}. The index 1 denotes Cu, 2 denotes O_x, and 3 denotes O_y.

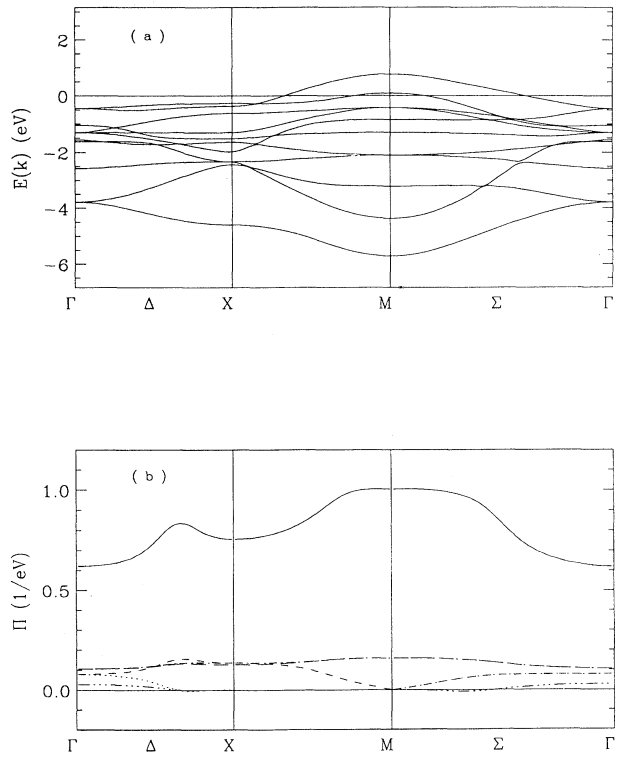

FIG. 3. (a) Electronic band structure as in the model from Fig. 2(a) but using reduced tight-binding parameters $V_{pd\sigma}$ and $V_{pd\pi}$. (b) Matrix elements $\pi_{\kappa\kappa'}(\mathbf{q})$ calculated with the band structure from (a).

parameters used) modulating dynamically the covalent bond between copper and the apex oxygen. On the other hand, the unstable tilt and rotational mode at the X point are not influenced at all by this electronic degree of freedom which means that a relative destabilization of the "ferroelectric mode" in comparison with these other instabilities in the system might be possible, i.e., ferroelectricity could overwhelm the X point instabilities in systems where dipolar fluctuations of the type considered can be excited easily. To be more definite, suitable candidates could be, for example, perovskites (ABO_3) where, on the one hand, hybridization of the (unoccupied) d states of the B cations with the oxygens is easily possible[29] and, on the other hand, there is simultaneously a large polarizability of the anion. Indeed, most ferroelectric perovskites based on oxygen fulfill these conditions.

Another interesting feature simultaneously develops in the above model together with the softening of the ferroelectric mode frequency, namely, a "rotonic" minimum shows up in the corresponding transverse acoustic mode in the Δ direction, see Fig. 4. We would like to mention that a possible occurrence of such a minimum, for example, in $SrTiO_3$, would be helpful for an interpretation of the phase-transition-like feature as discussed in this material in the quantum paraelectric regime.[18] Further, the appearance of such a minimum in the dispersion could be of some relevance for the occurrence of incommensurate modulated structures in the HTSC. Such a structure has been observed, for example, in the YBaCuO system[30] after substitution of boron for the chain copper. It might be possible that such replacement (besides the change in the long-range Coulomb interaction) could enhance the covalent hybridization and also the dipolar fluctuations at the apex oxygen.

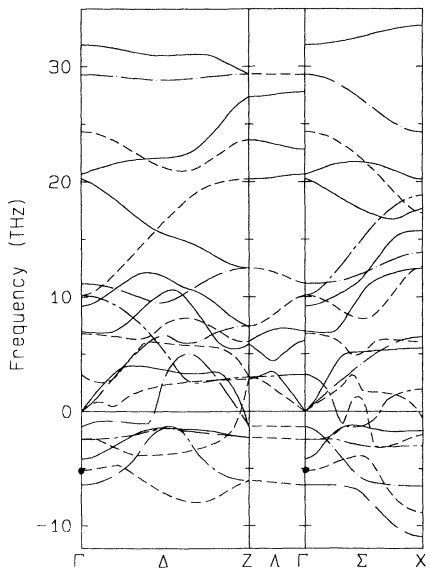

FIG. 4. Calculated phonon dispersion of tetragonal La_2CuO_4 in the ionic model using nominal charges for the ions and including additionally axial dipolar fluctuations at the apex oxygens. The dots indicate the unstable "ferroelectric mode."

The last topic of this section deals with a calculation of the phonon dispersion for La_2CuO_4 in the metallic phase under the assumption of a nonadiabatic electronic response. This means that the polarizability function [Eq. (9)] becomes frequency dependent via the energy denominator by adding $-(\hbar\omega+i\delta)$ where ω is the phonon frequency and δ an infinitesimal small positive real number ($\delta\rightarrow O$). The phonon frequencies then must be determined self-consistently from the secular equation which contains ω implicitly. In a "normal" three-dimensional (3D) metal and also for $\mathbf{q}$ orthogonal to the c direction in the HTSC one can neglect the phonon energy in the denominator of Eq. (9) and we are in the adiabatic regime. As mentioned earlier, the adiabatic description seems to be valid for La_2CuO_4 because of a sufficiently large c direction dispersion of the electronic bands. Actually we should then use a slightly three-dimensional model for the electronic band structure and the polarizability π, respectively, in order to be consistent with the adiabatic approximation. However, as long as we are in the adiabatic limit, a slight q_z dependence of π does not modify significantly the phonon dispersion in the metallic phase as compared to a purely two-dimensional polarizability. So we have used a two-dimensional model for π in our adiabatic phonon calculations.

However, the situation changes fundamentally if we are in the nonadiabatic regime [$\omega\neq 0$ in the denominator of Eq. (9) is taken into account], i.e., if the dispersion of the electronic bands in the c-direction becomes more and more two dimensional and in the end smaller than the phonon frequency for some phonons in the (0,0,1) direction. Finally, in the extreme limit of a strictly two-dimensional band structure the intraband contribution in π from Eq. (9) vanishes identically for phonons with wave vectors along the c direction (like O_z^z), exactly as it is the case in a two-dimensional insulator. This strongly reduced screening means, for example, that the A_{2u} discontinuities including the "ferroelectric split" do not vanish in the metallic phase, see Fig. 5(a), where we have displayed the results of the nonadiabatic phonon dispersion for the two-dimensional model of π. The dispersion in the Λ direction is that of a two-dimensional insulator [compare with Fig. 1(a) in this paper and 3(b) of Ref. 3], i.e., the O_z^z mode again becomes the highest Λ_1 mode at the Z point and the characteristic Λ_1 branch with the steep dispersion as obtained in the metallic phase within the adiabatic approximation has disappeared from the spectrum [compare with Fig. 5(b) where the results within the adiabatic approximation are displayed in the Δ, Λ, and Σ directions together with the nonadiabatic phonon dispersion along the $\Lambda'\sim(\varepsilon,\varepsilon,1)$ direction]. In the plot of Fig. 5(a) we have excluded the small-$q_{x,y}$ wave-vector regions around Γ and when approaching the Z point from the Δ direction. In these regions special nonadiabatic effects may occur which we have not investigated so far (e.g., coupling to acoustic plasmons near the Z point which will be investigated in more detail in future work). Exactly at the Γ point, however, the E_u splittings are virtually closed. Finally, the strongly reduced screening in the nonadiabatic limit leads to the large insulatorlike enhancement of the phonon-induced

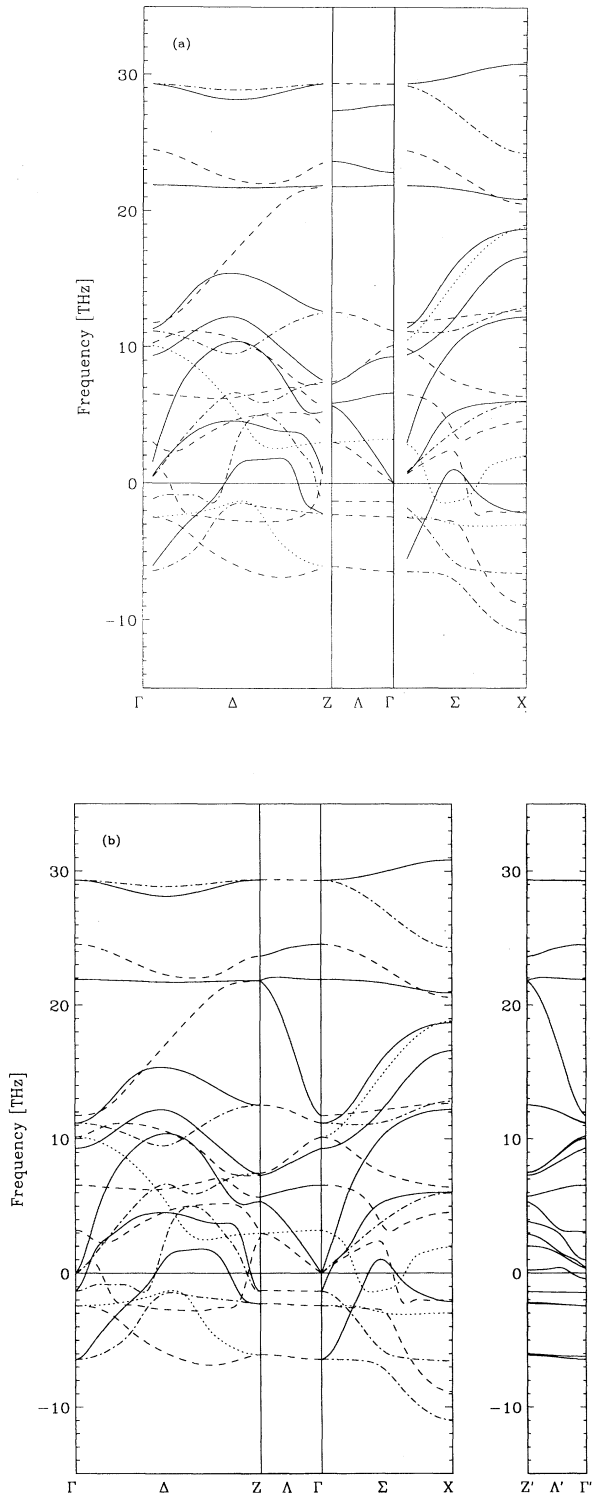

FIG. 5. Phonon dispersion of the metallic phase of tetragonal La_2CuO_4 taking nonadiabatic effects via the polarizability π into account (a). In (b) the corresponding results in the adiabatic approximation are given for the Δ, Σ, and Λ directions. Additionally we have included the nonadiabatic results along the $\Lambda' \sim (\varepsilon, \varepsilon, 1)$ direction. $\varepsilon = 0.05\pi/a$. The splitting of the Λ_3 modes is not visible in the plot for the two highest Λ_3 branches.

changes of the crystal potential in the CuO plane for high-frequency phonons in the Λ direction and, in particular, for O_z^z as discussed in the Introduction.

At this point we would like to mention that in case the adiabatic approximation really should break down for certain phonons in the (0,0,1) direction of the HTSC, nevertheless, the results calculated in the adiabatic approximation will remain meaningful at least outside a tube along the c direction with a certain radius depending on the magnitude of the dispersion of the electronic band structure in the $k_{x,y}$ plane such that the "adiabatic replacement" $\omega = 0$ in Eq. (9) is allowed. This also means that, in case the dispersion is decreased as in the band structure model of Fig. 3(a), the radius of the tube along the c direction increases and the phase space where nonadiabatic effects may become important increases too.

In order to demonstrate this matter explicitly, we have calculated the nonadiabatic phonon dispersion outside this tube, i.e., along, e.g., the $\Lambda' \sim (\varepsilon, \varepsilon, 1)$ direction with a small $\varepsilon = 0.05\pi/a$. The results are displayed in Fig. 5(b), and indeed, the dispersion is very similar like that of the adiabatic approximation along the Λ direction. In particular, the steep Λ_1 branch not present in the nonadiabatic calculation along the Λ direction [Fig. 5(a)] is clearly visible again. From these results we can also conclude that the adiabatic approximation is really valid for these phonons in the Λ direction if the $\mathbf{q}$ vector in the actual measurements[34,35] was along the Λ direction with high precision.

IV. La_2CuO_4 IN THE ORTHORHOMBIC PHASE

It is well known that when the temperature is lowered La_2CuO_4 undergoes a tetragonal-to-orthorhombic transition. Accompanying the orthorhombic distortion there are internal displacements which consist essentially of a rigid rotation of the CuO_6 octahedra around the $(1,\bar{1},0)$ tetragonal axis.[31] This displacement pattern corresponds to the freezing in of the X point tilt mode.

In the framework of our ionic *ab initio* model described in Sec. II, we have minimized the total energy according to Eq. (3) in the orthorhombic phase. The number of structural parameters entering the total energy doubles as compared with the tetragonal phase. In our calculation we have chosen the z coordinates of O_{xy}, O_z, and La, the x coordinates of O_z and La, and the three lattice constants a, b, and c. Further, the minimization has been done for the model using nominal ionic charges (denoted as "rigid ion" in Table II) and additionally for a model with the ionic configuration $Cu^{1.6+}$, $O^{1.6-}$, and $La^{2.4+}$ ("soft ion" in Table II).

The results for the structural parameters as obtained from the minimization of the energy in the two models are represented in Table II where they are compared with the so-called PIB model (potential induced breathing model[1,32]) and the experimental values.[31] From these data it can be extracted that our results are in good agreement with those of the PIB model. However, all ionic models overestimate the tilt effect significantly. The main reason is related to the fact that the tilt leads to a reduction of the overlap repulsion of the (spherical) ions

TABLE II. Structure parameters for orthorhombic La_2CuO_4 as obtained from the energy minimization for various models discussed in the text. The experimental results are from Ref. 31.

	a (Å)	b/a	c/a	$z(O_z)$	z(La)	$z(O_{x,y})$	$x(O_z)$	x(La)
Rigid ion	5.624	1.016	2.169	0.183	0.349	−0.060	0.135	0.0145
Soft ion	5.953	0.942	2.058	0.182	0.336	−0.045	0.119	−0.0046
PIB	5.742	1.016	2.14	0.183	0.350	−0.062	0.151	0.023
Expt.	5.371	1.008	2.43	0.187	0.362	−0.007	0.031	−0.007

and thus to a corresponding gain in energy.

The theoretical models also yield too large planar lattice constants and a too small c/a ratio. Similarly, as in the tetragonal phase, this deficiency can be traced back to the missing covalent contributions and the overestimation of the overlap repulsion between Cu and O_{xy} in the plane by the spherical ion approximation. Indeed, self-consistent LAPW-LDA calculations of the structural parameters for the tetragonal phase[1] lead to a better agreement with the experimental results. The small orthorhombicity expressed by the b/a ratio can be expressed quite well by the ionic models as can be seen in Table II. Further, the model with effective ionic charges predicts the correct direction of the movement of La in the x direction which is not the case for the PIB model and our model using nominal charges.

In order to point out how the two ionic models differ from each other it should be remarked that in the PIB model the ionic densities are additionally assumed to depend on the actual configuration of the ions via the Madelung potential, such that the radius of the Watson sphere varies with the Madelung potential when the ions are vibrating. However, both ionic models neglect the redistribution of the electronic charge density due to covalency, and in metals, due to the presence of a Fermi surface, i.e., metallic screening. On the other hand, using the ionic model only as a reference system to describe the dominant part of the local electronic density response as in our approach, these additional screening effects can be taken into account in an approximate way as described in Secs. II and III, respectively.

The phonon dispersion curves of the "rigid ion" and "soft ion" model from Table II are illustrated in Figs. 6(b) and 6(c), respectively, and compared with the results of the rigid ion model from Fig. 1(a) for tetragonal La_2CuO_4, which are displayed in the orthorhombic Brillouin zone for convenience [Fig. 6(a)]. In most experiments the tetragonal representation is used and so it is useful to give the relation between the two notations for the symmetry lines of the two Brillouin zones:

$$\Xi_o \equiv (\zeta,\zeta,0)_o \approx \Delta_t \equiv (\zeta,0,0)_t \ ,$$

$$\Lambda_o \equiv (0,0,\zeta)_o \approx \Lambda_t \equiv (0,0,\zeta)_t \ ,$$

$$\Delta_o \equiv (\zeta,0,0)_o \approx \Sigma_t \equiv (\zeta,\zeta,0)_t \ ,$$

$$\Sigma_o \equiv (0,\zeta,0)_o \approx \Sigma_t \equiv (\bar{\zeta},\zeta,0)_t \ .$$

Note also that the tetragonal X point is folded on the orthorhombic Γ point and Z point, respectively.

Comparing Figs. 6(a) and 6(b) we see that the width of the phonon spectrum is considerably smaller in the orthorhombic phase. There is a reduction of the highest frequency from about 34 THz in the model based on the tetragonal structure to about 27 THz in the orthorhombic one. A further reduction can be read off from Fig. 6(c) for the model with effective ionic charges where we obtain about 23 THz which is close to the experiment with about 21 THz.[33,34] The remaining 2 THz can be explained by screening via charge fluctuations. The inspection of Figs. 6(a)–6(c) further shows the splitting of the doubly degenerate Λ_3 mode of the tetragonal phase into Λ_2 and Λ_4 modes of the orthorhombic phase. Because of the overestimation of the tilt in our models this splitting should be too large. Also the inequivalence of the orthorhombic (1,0,0) and (0,1,0) directions is clearly visible from this comparison. The number of unstable modes, which are represented as negative frequencies, is strongly reduced in the orthorhombic phase in both models, compared with Fig. 6(a). Only modes which consist of a mixture of O_z and La sliding combined with a rotation around the c axis of O_x and O_y remain unstable in the orthorhombic phase, indicating that these modes will be very anharmonic. In particular, the unstable X point tilt mode of the tetragonal phase is stabilized in the orthorhombic structure. Because X_t is folded on Γ_o and Z_o we obtain two stable modes, one at Γ_o, $\nu=4.53$ THz (A_g), and the other at Z_o, $\nu=8.75$ THz (B_{1g}), for the model with nominal charges. These modes are also stable in the "soft ion" model, see Fig. 6(c). Likewise as in the tetragonal phase, Fig. 1(b), the frequency of the "ferroelectric mode" is decreased in case effective ionic charges are used (11.91 THz→10.59 THz).

The planar oxygen breathing mode at the X_t point whose large frequency is related to the strong ionic forces, as discussed in Ref. 3, still has nearly the largest frequency but the increasing dispersion of the corresponding phonon branch from Γ to X_t in tetragonal La_2CuO_4 (Fig. 1) gets lost, see the highest Δ_1 branch along Γ-Δ-$\Gamma(X_t)$ in Figs. 6(b) and 6(c). However, the correct behavior can be restored if the effects of charge fluctuations in the CuO plane are taken into account, see Sec. V. Finally, we mention the frequency change of the O_z^z mode from $\nu=27.37$ THz (tetragonal La_2CuO_4) to $\nu=25.97$ THz ("rigid ion") and $\nu=20.76$ THz in the "soft ion" model. As an interesting consequence of the orthorhombic tilt the displacements of the apex oxygens are no more exactly along the z direction in the O_z^z mode and, additionally, a second O_z^z-like mode at a lower frequency (19.92 and 15.79 THz, respectively) evolves from the "antitilt mode" B_{3g} at X_t (18.81 THz with nominal

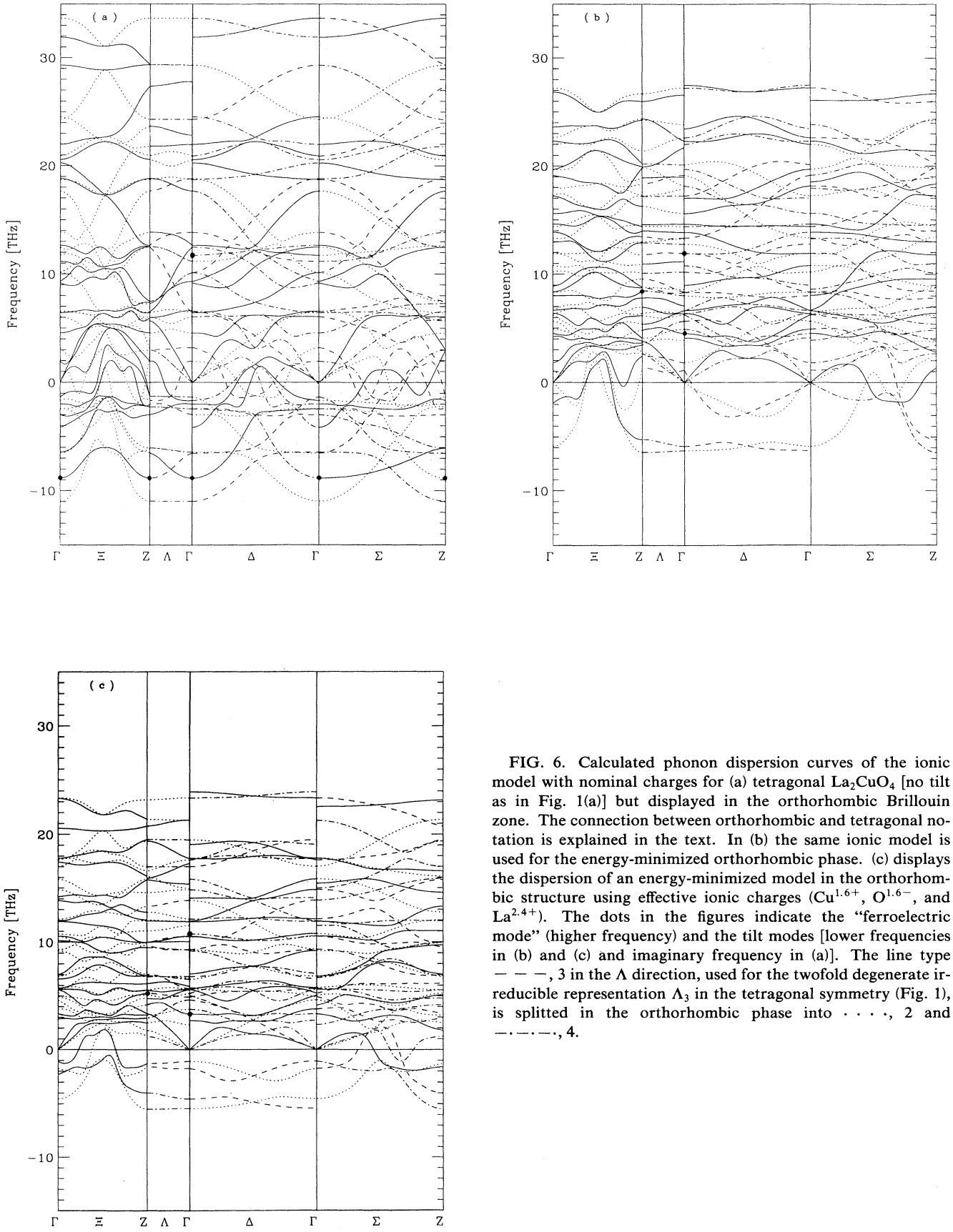

FIG. 6. Calculated phonon dispersion curves of the ionic model with nominal charges for (a) tetragonal La_2CuO_4 [no tilt as in Fig. 1(a)] but displayed in the orthorhombic Brillouin zone. The connection between orthorhombic and tetragonal notation is explained in the text. In (b) the same ionic model is used for the energy-minimized orthorhombic phase. (c) displays the dispersion of an energy-minimized model in the orthorhombic structure using effective ionic charges ($Cu^{1.6+}$, $O^{1.6-}$, and $La^{2.4+}$). The dots in the figures indicate the "ferroelectric mode" (higher frequency) and the tilt modes [lower frequencies in (b) and (c) and imaginary frequency in (a)]. The line type — — —, 3 in the Λ direction, used for the twofold degenerate irreducible representation Λ_3 in the tetragonal symmetry (Fig. 1), is splitted in the orthorhombic phase into · · · ·, 2 and —·—·—·, 4.

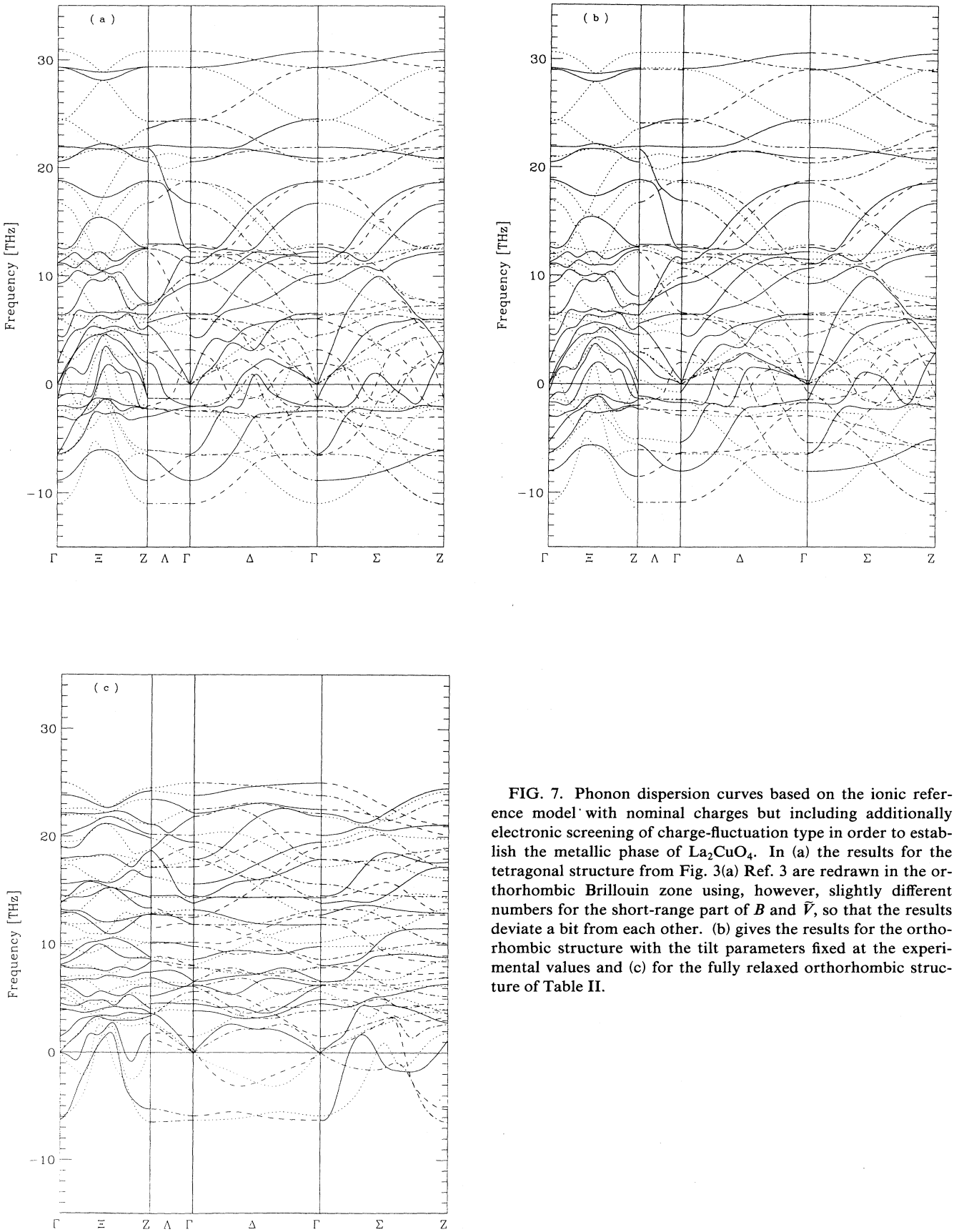

FIG. 7. Phonon dispersion curves based on the ionic reference model with nominal charges but including additionally electronic screening of charge-fluctuation type in order to establish the metallic phase of La_2CuO_4. In (a) the results for the tetragonal structure from Fig. 3(a) Ref. 3 are redrawn in the orthorhombic Brillouin zone using, however, slightly different numbers for the short-range part of B and $\tilde{V}$, so that the results deviate a bit from each other. (b) gives the results for the orthorhombic structure with the tilt parameters fixed at the experimental values and (c) for the fully relaxed orthorhombic structure of Table II.

charges) in the tetragonal phase. Such a mode would be able to induce qualitatively the same favorable charge-fluctuation pattern in the CuO planes as the original O_z^z mode. We come back to this point in the next section.

V. TILT AND NONLOCAL EPI EFFECTS OF CHARGE-FLUCTUATION TYPE

We investigate the influence of charge fluctuations on the phonon dispersion in the orthorhombic structure using the ionic model ["rigid ion," Fig. 6(b)] as a reference system. Then we discuss the relation between charge fluctuations and tilting.

In the same way as in Refs. 2 and 3 the electronic degrees of freedom (EDF) of charge-fluctuation type have been implemented in the model according to the formalism of Sec. II. These EDF simulate the screening effects in the HTSC beyond the ionic model. The different dielectric response in the metallic and the insulating phases of La_2CuO_4 is introduced using the criterion given by Eqs. (12a) and (12b).

The results for both the metallic as well as for the insulating phase are displayed in Figs. 7 and 8, respectively. In Fig. 7(a), we have shown the results for tetragonal La_2CuO_4 and displayed them in the orthorhombic Brillouin zone in order to isolate the features which are related to the folding of the two Brillouin zones. Figure 7(a) can be directly compared with Fig. 3(a) from Ref. 3 where the results are displayed in the tetragonal zone and also with Fig. 5(b). The main differences in the two plots can be understood by remembering that X_t is folded back on Γ_o and Z_o. This explains the "new" branches appearing in the orthorhombic zone scheme. For example, the splitting of the Λ_1 branch with the steep dispersion in Fig. 3(a) of Ref. 3 and Fig. 5(b) which recently has been observed experimentally[34] is such a folding effect.

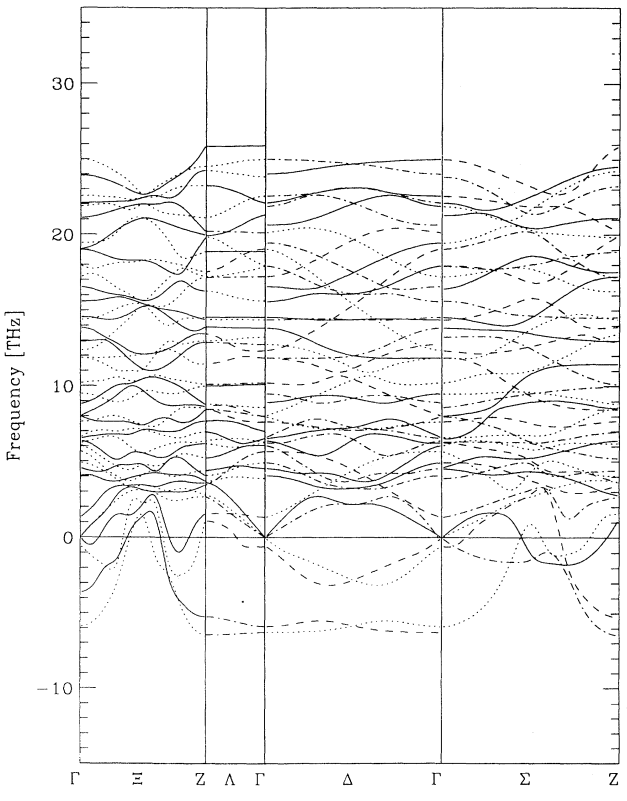

FIG. 8. Phonon dispersion for orthorhombic La_2CuO_4 based on the "rigid ion" model from Fig. 6(b) with nominal ionic charges but including additionally electronic screening by charge fluctuations restricted by the insulator conditions from Eqs. (12a) and (12b).

While the results shown in Figs. 7(c) and 8 are based on the "rigid ion" model from Fig. 6(b), which overestimates the tilt effect as discussed earlier, the dispersion curves in Fig. 7(b) have been obtained by fixing the tilt parameters $z(O_{xy})$, $x(O_z)$, and $x(La)$ to their experimental values but allowing the remaining five structural parameters to relax in the total-energy minimization. The results are $a=5.638$ Å, $b/a=0.997$, $c/a=2.126$, $z(O_z)=0.1897$, and $z(La)=0.363$.

Comparing Fig. 7(c) with Fig. 6(b) we see that the highest frequency in the spectrum is decreased by about 2 THz as a consequence of the screening via charge fluctuations. The increasing dispersion of the highest Δ_1 branch (in the Γ-Δ-Γ direction) including the planar oxygen breathing mode has been restored by the charge fluctuations in the metallic as well as in the insulating phase in agreement with the experiments.[33,34] From Fig. 7 we extract that all phonon branches are continuous at Γ (no LO-TO splittings or discontinuities) which is a consequence of the metallic screening and this is completely different in the ionic models or in Fig. 8, where such discontinuities arise because of the energy gap in the electronic spectrum. Also the Λ_1 branch with the steep dispersion in the metallic phase is not present in the insulating phase in agreement with experiment.[35] As discussed in detail in Refs. 2 and 3 and mentioned earlier this branch appears in the metallic phase as a consequence of the vanishing of the large A_{2u} discontinuity of the "ferroelectric mode" because of the metallic screening via charge fluctuations in the adiabatic approximation. The inequivalence of the dispersion in the (1,0,0) and (0,1,0) directions and the splitting of the tetragonal Λ_3 branch into two nondegenerate branches Λ_2 and Λ_4 in the orthorhombic structure apparently follows from the inspection of Figs. 7(b) and 7(c) when compared with Fig. 7(a). These effects are large in Fig. 7(c) because of the overestimation of the tilt in this model and only weakly developed in the model with the fixed tilt corresponding to Fig. 7(b).

From our calculations we also obtain values for the infrared active phonons. A comparison of the calculated frequencies within the model using nominal ionic charges (N) and the model with effective ionic charges (S) are listed in Table III. Comparison is made with several experimental sources.[36–38] The A_{2u} modes in tetragonal notation correspond to B_{1u} in the orthorhombic notation while E_u tetragonal corresponds to B_{2u} and B_{3u} orthorhombic. The apex oxygen bending mode[36] has not been observed in the experiments, see Table III.

Table IV contains the results for the charge fluctuations induced by the A_g modes at the Z point on the Cu

TABLE III. Calculated values for the infrared-active phonons within the model using nominal ionic charges (N) and also for the model with effective ionic charges (S). Comparison is performed with several experimental sources (expt. 1, Ref. 36; expt. 2, Ref. 37; expt. 3, Ref. 38). The frequencies are given in THz.

	Tetrag. $A_{2u}\sim$ ortho. B_{1u}				Tetrag. $E_u\sim$ortho. B_{2u},B_{3u}		
N	6.15	11.87	21.88	3.88	8.60	15.63	23.83
S	5.60	10.63	17.80	2.32	6.70	11.95	21.28
Expt. 1				4.34		10.79	20.83
Expt. 2	7.25	10.25	15.02	3.96		10.73	19.99
Expt. 3		9.59	15.02	4.86		10.88	20.11

and the $O_{x,y}$ ions in the CuO plane as calculated for several models according to Eq. (21) of Ref. 3. The model denoted as OT represents the results in the tetragonal structure (zero tilt) for metallic La_2CuO_4. Only the tetragonal $A_g(Z)$ modes (O_z^z, 21.95 THz and La_z^z, 5.43 THz) couple to the charge fluctuations in this case, whereas the tetragonal-$B_{3g}(X)$ modes do not. The calculated values deviate a bit from the corresponding results in Table II of Ref. 3 because we have used slightly different numbers for the short-range part of B and $\tilde{V}$ in both calculations. As can be seen from Table IV and following the discussion in Ref. 3, the O_z^z and to a lesser extent the La_z^z vibration induce charge fluctuations at the Cu and $O_{x,y}$ that have the same sign in the whole plane. This finally leads to charge fluctuations of alternating sign in consecutive planes ("interplane charge transfer") which provide the screening mechanism for the long-range Coulomb interactions, being responsible for the high frequency of O_z^z in the insulating model (IN$\rightarrow$25.85 THz) and the ionic model (25.97 THz). Thus, compared with the ionic model, we have a strong renormalization of O_z^z in the metal (at least within the adiabatic approximation underlying these calculations) but virtually no decrease in frequency for O_z^z in the insulating model, where the interplane charge transfer, characteristic for screening in the metallic phase, is blocked completely. We obtain in this case only charge fluctuations compensating each other locally within the CuO plane, and this is less effective for screening, see model IN in Table IV. Turning to the tilted structure (models IN, MN, MS, 1T) we see that even the former tetragonal $B_{3g}(X)$ modes now couple to the charge fluctuations as a consequence of the tilt. Moreover, an inspection of the data for the charge fluctuations in the models MN, MS, and 1T in Table IV, all of which describe the metallic phase of orthorhombic La_2CuO_4, demonstrates that the charge fluctuations have the same sign at all ions in the CuO plane at least for four of the five A_g modes. In the case of the A_g mode with the lowest frequency in the models MN and MS the sign is not the same, however, the charge fluctuations at the $O_{x,y}$ ions clearly dominate those at Cu, so that this mode also generates interplane charge transfer. In other words, instead of the two modes O_z^z and La_z^z in the tetragonal structure in the orthorhombic structure we now have five modes inducing at least qualitatively the same favorable charge-fluctuation pattern being important for pairing via nonlocal EPI as discussed in Ref. 3.

A more detailed analysis of the situation shows that, in particular, a second O_z^z-like mode ($O_z^{z'}$) evolves as a result of the tilt, which could be very effective in producing the favorable charge fluctuations just discussed in case the magnitude of the tilt would be large enough as it is, e.g.,

TABLE IV. Phonon frequencies ν in THz, z component of the eigenvector of the O_z and La atoms $e_z^{O_z}$, e_z^{La}, and charge fluctuations $\delta\zeta$ according to Eq. (21) in Ref. 3 at Cu, O_x, and O_y for the A_g modes at the Z point. The eigenvectors are normalized to one. Negative values of $\delta\zeta$ correspond to an increase of electronic charge at the ions. The unit of $\delta\zeta$ is 10^{-3}. $e_z^{O_z}>0$ ($e_z^{La}>0$) means that O_z (La) is moving away from Cu. All models given in the table (except the model denoted as MS), are based on nominal ionic charges. MS denotes the model for the metallic phase based on effective ionic charges [Fig. 6(c)]. IN denotes the model for the insulating phase (Fig. 8), MN means the metallic phase [Fig. 7(c)]. OT denotes the results for the tetragonal structure, compare with Ref. 3 and Fig. 7(a), and 1T represents the results keeping the tilt fixed at the experimental value [Fig. 7(b)]. The * indicates the original O_z^z and La_z^z modes already present in the tetragonal structure, i.e., the axial O_z and La_z breathing modes at the Z point, see results for OT.

	ν	$e_z^{O_z}$	e_z^{La}	$\delta\zeta$(Cu)	$\delta\zeta(O_x)$	$\delta\zeta(O_y)$
IN	3.61	0.14	0.46	−5.88	2.94	2.94
	7.69*	0.04	0.07	−4.18	2.09	2.09
	13.91	0.12	0.07	3.30	−1.65	−1.65
	19.92	0.16	−0.01	0.30	−0.15	−0.15
	25.85*	0.44	−0.17	−4.52	2.26	2.26
MN	3.63	0.13	0.47	−1.97	3.47	3.47
	7.45*	0.00	0.08	2.06	5.26	5.26
	12.80	−0.02	0.09	11.26	6.63	6.63
	18.77	0.41	−0.08	−10.44	−8.82	−8.82
	21.14*	0.25	−0.11	−10.15	−7.08	−7.08
MS	3.20	0.12	0.46	−1.40	3.22	3.22
	5.93*	0.02	0.14	1.75	4.07	4.07
	9.39	0.01	0.09	8.18	3.83	3.83
	14.86	0.37	−0.06	−8.94	−7.22	−7.22
	17.30*	0.31	−0.11	−9.55	−6.75	−6.75
OT	−2.99	0.0	0.0	0.0	0.0	0.0
	1.94	0.0	0.0	0.0	0.0	0.0
	5.43*	0.12	0.49	1.32	5.84	5.84
	18.81	0.0	0.0	0.0	0.0	0.0
	21.95*	0.49	−0.12	−14.35	−11.13	−11.13
1T	−1.09	0.01	0.01	2.50	0.04	0.04
	2.51	0.00	−0.02	2.57	1.12	1.12
	5.40*	0.12	0.49	1.40	5.87	5.87
	18.87	0.07	−0.01	−1.76	−1.47	−1.47
	21.95*	0.48	−0.12	−14.24	−11.07	−11.07

the case in the MN model in Table IV ($O_z^{z'} \rightarrow 18.77$ THz, see also Fig. 9). However, from our discussion in Sec. IV we know that this model overestimates the tilt effect and we think that the results which follow from the model with the experimental tilt (1T) are more appropriate, see Table IV and Fig. 9. As mentioned earlier, the $O_z^{z'}$ mode evolves from the "antitilt mode" at X_t (A_g mode at 18.81 THz in the OT model shown in Fig. 9). In the orthorhombic structure, the eigenvector of the apex oxygen then gets a z component due to the occurrence of the tilt, which depends on both the magnitude of the tilt and the screening properties (insulator or metal) of the material. Comparing in Table IV the calculated data for $O_z^{z'}$ in the IN model with those of the MN model we find that the z component is larger in the metallic phase, see also Fig. 9.

From the experiments reported in the literature[12–16] it is evident that for La_2CuO_4 not only the hole content is important for superconductivity but that there is also a relationship between superconductivity and several structural changes. Recently, it was reported in Ref. 15 that the superconductivity in overdoped $La_{2-x}Sr_xCuO_4$ belongs only to the orthorhombic structure and not to the tetragonal. It is tempting to discuss this finding which, however, is not supported by the results given in Ref. 16 (see below) on the basis of the results obtained for the charge fluctuations (Table IV) and corresponding changes in the crystal potential favoring phonon-mediated pair binding. In particular, we can read off from this table the changes of these fluctuations induced by the tetragonal-to-orthorhombic transition and we see that they are favored by the tilt. However, in order to assign unequivocally a preference to the orthorhombic phase from this point of view the tilt should be large enough as it is, for example, the case for the MN model. On the other hand, the experimental tilt is much smaller and so the results for the 1T model seem to be more suitable. From these data a clearcut preference of the orthorhombic phase cannot be derived by comparing with the OT model, i.e., with the data as obtained in the tetragonal phase. Thus, superconductivity intrinsic to the tetragonal structure cannot be ruled out on the basis of the charge fluctuations. This would be consistent with the experimental results in Ref. 16 where superconductivity has been observed in the pressure-stabilized tetragonal structure. In this context one should note that the apex oxygen could move towards the CuO plane with increasing hydrostatic pressure (as it is found in Ref. 39 for $YBa_2Cu_4O_8$), a fact which would increase the charge fluctuations induced by the modes above and thus could lead to an increase of T_c with pressure at fixed doping. Changing the doping rate, on the other hand, influences the charge fluctuations explicitly and also implicitly via the variation of the tilt angle.

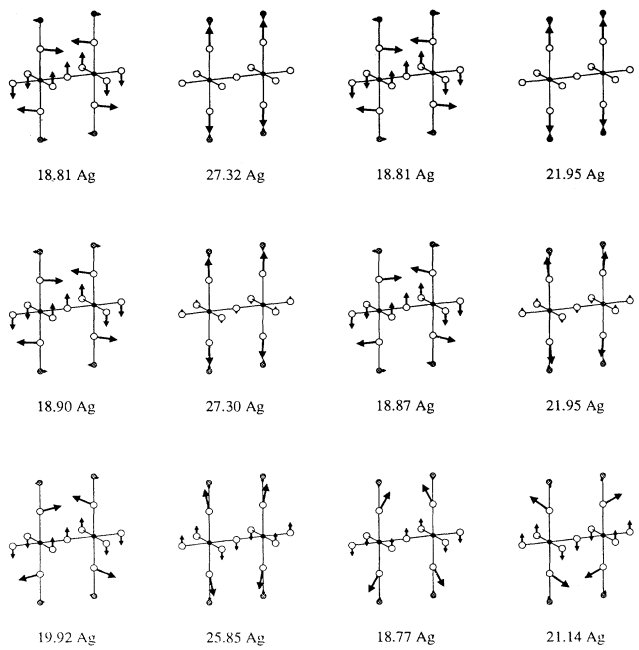

FIG. 9. Displacements of the atoms in the axial breathing modes of the apex oxygens (O_z^z and $O_z^{z'}$). The first two columns represent the insulating phase and the last two columns the metallic phase. The first row is the results for the tetragonal structure from Ref. 3 (OT). The second row corresponds to "fixed tilt" (1T) as in Fig. 7(b). The third row displays the results for the models denoted as IN and MN in Table IV [Figs. 8 and 7(c)].

VI. NONLOCAL EPI AND OPTIMAL CONCENTRATION FOR DOPING

The last topic to be discussed in this paper is of more general nature. It deals with an interpretation of a universal relationship between the hole content p (number of holes per CuO_2 unit in the CuO layer) and the transition-temperature T_c among the HTSC. In Ref. 19, on the basis of an analysis of the experimental data, such a universal relation between $T_c/T_{c,\max}$ and the hole concentration in the CuO plane has been established. This relation is characterized by sharp bends at $p \approx 0.06$, 0.12, 0.25, and 0.31 which correspond to the onset of superconductivity, the beginning and the end of a T_c plateau where $T_c/T_{c,\max}=1$, and the disappearance of superconductivity, respectively. These values for the hole content are related to ordered arrangements of holes in the CuO plane.[19] Hole contents with $p=0.0625$, 0.125, 0.25, and 0.3125 correspond to distances $4a$, $2\sqrt{2}a$, $2a$, and $\sqrt{2}a$ between two nearest-neighboring holes and it can be seen that the hole contents calculated from the ordered arrangements of holes are in very good agreement with the critical p values of the universal relationship.

In the case when only local EPI is considered, because of the time retardation $\pi/2\omega$ (ω is the phonon frequency times 2π), we get a single "optimal length" $\xi=\pi v_f/2\omega$ (v_f is the Fermi velocity) for the electrons (holes) of the pair interacting locally via the same atom. This distance is of the order of magnitude of the spatial extension of the pair. On the other hand, taking into account nonlocal EPI effects of charge-fluctuation type as discussed in context with the O_z^z mode, we obtain for a given frequency a continuous distribution of "optimal lengths" for pairing whose range is between $\xi_{\min}=\xi-d_{\rm nl}$ and $\xi_{\max}=\xi+d_{\rm nl}$. Here $d_{\rm nl}$ denotes the diameter of the area

of nonlocality generated by the charge fluctuations in the CuO plane if, for example, an apex oxygen ion is displaced. The value for d_{nl} is $1a$, where a (≈ 4 Å) is the planar lattice constant for the high-T_c cuprates. Estimating for $\zeta \sim 12$ Å $\approx 3a$ (note that one can expect a very short length for ζ in the HTSC due to their low Fermi velocities and high T_c values) we obtain possible values between $\zeta_{max}=4a$ and $\zeta_{min}=2a$. ζ_{max} then determines a critical lower hole content $P_c^{min}=0.0625$ because the average distance between the holes should be smaller than ζ_{max}, otherwise the favorable situation for pairing via an "optimal length" is not possible. Comparing with the result from the universal curve our P_c^{min} is in good agreement with the onset of superconductivity at $p=0.06$. In case the smallest distance d_{nn} between two holes fulfills $d_{nn} \geq \zeta_{min}$, all holes with distances between d_{nn} and ζ_{max} can contribute to optimal pairing within the charge-fluctuation mechanism. With decreasing d_{nn} ($\geq \zeta_{min}$) the number of holes which will be active in pairing via an "optimal length" increases, but, on the other hand, the Coulomb repulsion between the holes increases too and counterworks the pairing. This is very likely to result in a plateaulike feature. Obviously, the range of steep increase in T_c followed by the T_c plateau in the universal curve ($0.25 \geq p \geq 0.06$) corresponds to the interval $\zeta_{min} \leq d_{nn} \leq \zeta_{max}$ ($0.25 \geq p \geq 0.0625$) and the beginning of the plateau at $p=0.12$ can be associated with $d_{nn}=\zeta$ ($p=0.11$). Finally, if d_{nn} decreases further below ζ_{min} we will obtain at ζ_{min} an upper critical hole content $P_c^{max}=0.25$ favorable for pairing because the holes with the shortest distances (from d_{nn} up to just below ζ_{min}) no longer contribute to pairing via an "optimal length" while, on the other hand, the Coulomb repulsion between the holes further increases leading effectively to a suppression of pairing for higher concentrations than $P_c^{max}=0.25$. Our value for P_c^{max} is in full agreement with the result from the experiments.

VII. SUMMARY

In the following we collect the main results of the paper. We have studied the role of bonding, reduced screening, and of structural aspects in the HTSC using La_2CuO_4 as an example. In addition to our calculations in Refs. 2 and 3 for the tetragonal phase of La_2CuO_4 based on an ionic *ab initio* model complemented by screening via charge fluctuations we have estimated the influence of covalency on the structural parameters and the phonon dispersion within a simple model. We find an improvement of the structural parameters in comparison with the ionic model. In particular, the planar lattice constant can be decreased by covalence effects and two unstable E_u modes and an E_g mode of the ionic model are remarkably stabilized.

Narrowing of the electronic band structure as motivated by the calculations in Ref. 17 leads to an enhancement of the Cu-Cu polarizability and to a broadening of the nesting peak at the $M(X)$ point but has only little influence on the phonon dispersion in adiabatic approximation. On the other hand, the phase space where nonadiabatic effects may become important is increased by such a narrowing.

Our considerations concerning the "ferroelectric mode" in La_2CuO_4 have shown that the stability of this mode in this material is mainly due to the strong short-range overlap repulsion between the ions. In studying possible microscopic mechanisms which would favor the tendency towards ferroelectricity we have isolated axial dipolar fluctuations at the apex oxygens as the driving force. Simultaneously, a "rotonic" minimum shows up in the corresponding acoustic branch.

We have pointed out that caution may be required when using the adiabatic approximation in the HTSC because of their quasi-two-dimensional electronic structure. We have demonstrated that nonadiabaticity leads to a strongly reduced screening in the metallic phase for phonons with wave vectors in the c direction and a behavior as in a two-dimensional insulator occurs if the electronic structure would be strictly two dimensional. This leads to large nonlocal changes in the crystal potential in the CuO plane induced by phonons in the (0,0,1) direction, like O_z^z, and to a reinforcement of the nonlocal pairing mechanism proposed in Refs. 2 and 3.

We then focused our interest on effects related to the tetragonal-to-orthorhombic phase transition. We have performed energy minimizations and found good agreement for the structure parameters in our ionic model with the results as obtained with the PIB model. However, all ionic models overestimate the tilt effect. The main effect of the tilt on the phonon dispersion which has been found is to reduce the width of the spectrum considerably. In the model where effective ionic charges are used the calculated width approaches the experimental results quite well. The difference of about 2 THz can be explained by screening via charge fluctuations. The number of unstable modes is strongly reduced in the orthorhombic structure and only modes which consist of a mixture of O_z and La sliding motion combined with a rotation of O_x and O_y around the c axis remain unstable indicating the anharmonicity of these phonons. Further, we have given values for the infrared-active phonons and performed a comparison with the available experimental data.

Another interesting consequence of the tilt has been pointed out, namely, the appearance of a second O_z^z-like mode at a lower frequency. This mode has been shown to induce qualitatively the same favorable charge fluctuations in the CuO plane like O_z^z itself. Altogether we find (instead of the two modes O_z^z and La_z^z in the tetragonal structure) five A_g modes in the orthorhombic phase inducing at least qualitatively the same favorable charge fluctuations and corresponding changes of the crystal potential. However, in the model where in agreement with experiment a small tilt is realized the contribution found for the original O_z^z mode also present in the tetragonal phase dominates by far. Thus, from this point of view there is no clearcut preference of the orthorhombic structure as being of exceptional importance for superconductivity and the possibility that this phenomenon can also be intrinsic to the tetragonal structure cannot be ruled out.

Finally, in the last topic we have presented on the basis of the nonlocal electron-phonon interaction mechanism of charge-fluctuation type a theoretical explanation of a universal relation between T_c and the hole content in the CuO plane of the HTSC.

Note added in proof

A further remark in context with nonadiabatic effects is appropriate at this place. In case there is a sufficiently small dispersion of the electronic band structure in the c direction at the Fermi level we may look for low-lying plasmon modes along the Λ direction which will couple to the O_z^z and La_z^z phonon at the Z point and (mainly) to the ferroelectric mode at Γ. At the moment our preliminary calculations show that in Λ direction a plasmon excitation (starting at zero frequency in the two-dimensional case) is pushed through the phonon spectrum if the dispersion of the electrons in the c direction is increased in our model. This low-lying plasmon interacts strongly with the phonons mentioned above leading to mode coupling. In this way besides a renormalized phononlike mode a plasmonlike extra mode appears at low frequencies.

For a very small electronic dispersion in the c direction the plasmonlike mode is lower than the phononlike mode (phonons contribute in this case substantially to the screening of the plasma oscillations; antiadiabatic limit) while the situation is reversed in case the dispersion is increased (electrons start to follow more effectively the motion of the ions). Now the plasmonlike mode is higher in frequency than the phononlike mode and the latter can be assigned to the Λ_1 mode with the steep dispersion. Increasing the dispersion of the electrons in the c direction still further towards the adiabatic regime this mode finally approaches its adiabatic shape [Fig. 5(b)] from below. Note that the ferroelectric split is thus also closed from below. In any case, we obtain for a small enough dispersion of the band structure in the c direction a plasmonlike extra branch along Λ (with frequencies in the range of the frequencies of the phonons and of the superconducting gap region) which additionally will contribute to the pairing in the plane.

ACKNOWLEDGMENT

Financial support by the Deutsche Forschungsgemeinschaft is gratefully acknowledged.

[1]W. E. Pickett, Rev. Mod. Phys. **61**, 433 (1989).
[2]C. Falter, M. Klenner, and W. Ludwig, Phys. Lett. A **165**, 260 (1992).
[3]C. Falter, M. Klenner, and W. Ludwig, Phys. Rev. B **47**, 5390 (1993).
[4]H. Krakauer, W. E. Pickett, and R. E. Cohen, Phys. Rev. B **47**, 1002 (1993).
[5]T. Jarlborg, Phys. Lett. A **164**, 345 (1992).
[6]W. E. Pickett, H. Krakauer, R. E. Cohen, and D. J. Singh, Science **255**, 46 (1992).
[7]A. Svane, Phys. Rev. Lett. **68**, 1900 (1992).
[8]J. Ranninger, Z. Phys. B **84**, 167 (1991).
[9]S. N. Putilin, E. V. Antipov, O. Chmaissem, and M. Marezio, Nature **362**, 226 (1993).
[10]C. Falter, M. Klenner, Q. Chen, and W. Ludwig, Solid State Commun. **88**, 87 (1993).
[11]M. Klenner, C. Falter, and Q. Chen (unpublished).
[12]J. D. Axe, A. H. Moudden, D. Hohlwein, D. E. Cox, K. M. Mohanty, A. R. Moodenbaugh, and Youwen Xu, Phys. Rev. Lett. **62**, 2751 (1989).
[13]M. K. Crawford, R. L. Harlow, E. M. Mc Carron, W. E. Farneth, J. D. Axe, H. Chou, and Q. Huang, Phys. Rev. B **44**, 7749 (1991).
[14]N. Momono, M. Ido, M. Oda, N. Yamada, A. Onodera, Y. Okajima, and K. Yamaya, Physica C **183**, 241 (1991).
[15]H. Tagaki, R. J. Cava, M. Marezio, B. Batlogg, J. J. Krajewski, W. F. Peck, Jr., P. Bordet, and D. E. Cox, Phys. Rev. Lett. **68**, 3777 (1992).
[16]N. Yamada and M. Ido, Physica C **203**, 240 (1992).
[17]G. Dopf, J. Wagner, P. Dietrich, A. Muramatsu, and W. Hanke, Phys. Rev. Lett. **68**, 2082 (1992).
[18]K. A. Müller, W. Berlinger, and E. Tosatti, Z. Phys. **84**, 277 (1991).
[19]H. Zhang and H. Sato, Phys. Rev. Lett. **70**, 1697 (1993).
[20]F. Herman and S. Skillman, *Atomic Structure Calculations* (Prentice-Hall, Englewood Cliffs, NJ, 1963).
[21]J. P. Perdew and A. Zunger, Phys. Rev. B **23**, 5048 (1981).
[22]R. E. Watson, Phys. Rev. **111**, 1108 (1958).
[23]R. G. Gordon and Y. S. Kim, J. Chem. Phys. **56**, 3122 (1972).
[24]J. M. Longo and P. M. Raccah, J. Solid State Chem. **6**, 526 (1973).
[25]B. Piveteau and C. Noguera, Phys. Rev. B **43**, 493 (1991).
[26]H. Krakauer, W. E. Pickett, and R. E. Cohen, J. Supercond. **1**, 111 (1988).
[27]R. E. Cohen, W. E. Pickett, H. Krakauer, and D. A. Papaconstantopoulos, Phase Trans. **22**, 167 (1990).
[28]W. E. Pickett, R. E. Cohen, and H. Krakauer, Phys. Rev. Lett. **67**, 228 (1991).
[29]R. E. Cohen, Nature **358**, 136 (1992).
[30]J. Q. Li, W. J. Zhu, Z. X. Zhao, and D. L. Yin, Solid State Commun. **85**, 739 (1993).
[31]V. B. Grande, H. Müller-Buschbaum, and M. Schweizer, Z. Anorg. Allg. Chem. **428**, 120 (1977).
[32]R. E. Cohen, W. E. Pickett, L. L. Boyer, and H. Krakauer, Phys. Rev. Lett. **60**, 817 (1988).
[33]L. Pintschovius, in *Phonons 89,* Proceedings of the Third International Conference on Phonon Physics, edited by S. Hunklinger, W. Ludwig, and G. Weiss (World Scientific, Singapore, 1990), Vol. 1, p. 217.
[34]L. Pintschovius, N. Pyka, W. Reichardt, A. Yu. Rumiantsev, N. L. Mitrofanov, A. S. Ivanov, G. Collin, and P. Bourges, Physica C **185-189**, 156 (1991).
[35]L. Pintschovius, N. Pyka, W. Reichardt, A. Yu. Rumiantsev, A. Ivanov, and N. L. Mitrofanov (unpublished).
[36]S. Tajima, T. Ido, S. Ishibashi, T. Itoh, H. Eisaki, Y. Mizuo, T. Arima, H. Takagi, and S. Uchida, Phys. Rev. B **43**, 10496 (1991).
[37]R. T. Collins, Z. Schlesinger, G. V. Chandrashekhar, and M. W. Shafer, Phys. Rev. B **39**, 2251 (1989).
[38]F. Gervais, P. Echegut, J. M. Bassat, and P. Odier, Phys. Rev. B **37**, 9364 (1988).
[39]E. Kaldis, P. Fischer, A. W. Hewat, E. A. Hewat, J. Karpinski, and S. Rusiecki, Physica C **159**, 668 (1989).